Molecular complexes of small alkanes with Co+

ARTICLE *in* THE JOURNAL OF PHYSICAL CHEMISTRY · MAY 1993

Impact Factor: 2.78 · DOI: 10.1021/j100122a012

3 AUTHORS:

Jason K Perry
Gilead Sciences
37 PUBLICATIONS **2,913** CITATIONS
SEE PROFILE

Gilles Ohanessian
French National Centre for Scientific Research
115 PUBLICATIONS **3,673** CITATIONS
SEE PROFILE

William A. Goddard
California Institute of Technology
1,329 PUBLICATIONS **67,304** CITATIONS
SEE PROFILE

Molecular Complexes of Small Alkanes with Co^+

Jason K. Perry,† Gilles Ohanessian,‡ and William A. Goddard III*,†

Materials and Molecular Simulation Center, Beckman Institute (139-74), Division of Chemistry and Chemical Engineering,§ California Institute of Technology, Pasadena, California 91125, and Laboratoire des Mecanismes Reactionnels, Ecole Polytechnique, 91128 Palaiseau Cedex, France

Received: December 2, 1992; In Final Form: February 16, 1993

Using ab initio methods, including extensive electron correlation, we studied the molecular complexes of Co^+ with H_2 and a number of small alkanes (CH_4, C_2H_6, and C_3H_8). We found that the bond energies increase with ligand size, ranging from 17.2 (for $Co(H_2)^+$) to 29.3 kcal/mol (for $Co(C_3H_8)^+$), in close agreement with recent experiments. For methane, Co^+ coordinates to either two or three C–H bonds, with the η^2 geometry more stable by 1.3 kcal/mol out of 21.4 kcal/mol. For ethane, η^2 and η^3 coordinations of Co^+ to the C–H bonds are also favorable, but these bonds can be on either the same carbon center or different centers (strict coordination to the C–C bond was not found). Adding a second CH_4 to $Co(CH_4)^+$, we found that the second bond is *stronger* than the first by 1.7 kcal/mol. In addition, with both methanes in the η^2 configuration, we found that the C–H bonds are eclipsed (8.3 kcal/mol better than the staggered conformation). With both methanes in the η^3 configuration, however, they are staggered.

Introduction

In the past decade, a close collaboration between theory and experiment has brought to light a great deal of interesting chemistry involving transition-metal ions.[1] Much of the work has concerned the activation of C–C and C–H bonds of various hydrocarbons[2-7]—reactions of vital interest for real and potential analogues in homogeneous catalysis.[8] Kinetic studies[2] of these reactions have clearly illustrated that the chemistry of the transition series is quite varied, and thermochemical studies[7,9] have shown that a number of key metal–ligand bond energies (such as the metal hydrides) behave nonmonotonically across the first two transition-metal rows. Theory has illuminated the nature of this behavior as primarily due to atomic-state splittings and loss of metal-exchange energy.[10,11] Despite the wide range of chemistry observed, some trends can be discerned. One important trend is that the larger the alkane, the more reactive it is to transition-metal ions. As an example, Co^+ is unreactive toward CH_4 and C_2H_6, slowly eliminates H_2 and CH_4 from C_3H_8, and rapidly eliminates the same products from n-C_4H_{10}.[2,4] It is generally believed that this trend, which is illustrated in Figure 1 for Co^+ reacting with C_2H_6 and C_3H_8, is due at least in part to the increasing strength of the predissociation molecular complex.[6] As the first step along the reaction pathway involves oxidative addition to a C–H bond, it is assumed that the barrier to insertion is relatively constant for all alkanes. It is then the depth of the well for the molecular complex which determines whether the barrier lies above or below the dissociation threshold. Thus, $Co(C_2H_6)^+$ may not have enough energy to overcome the barrier to insertion, but $Co(C_3H_8)^+$ does (for $Co^+ + C_2H_6$, the deficit in energy for surmounting this barrier is <1 eV and perhaps substantially less;[4a,b] for $Co^+ + C_3H_8$, the barrier lies 0.11 ± 0.03 kcal/mol below the dissociation threshold[6]). While reactions of Co^+ with small alkanes have been well studied in terms of kinetics, a quantitative description of these potential energy surfaces is only now beginning to emerge.

Recent gas-phase equilibrium measurements by Kemper, Bowers, and co-workers[12,13] led to the determination of accurate complexation energies for atomic Co^+ with H_2,[12] CH_4, and C_2H_6.[13] The bond dissociation energies (BDEs) from these experiments were found to be 18.2 ± 1.0, 22.9 ± 0.7, and 28.0 ± 1.1 kcal/mol, respectively. Similar results were achieved by Haynes and Armentrout[14] for complexation of CH_4, C_2H_6, and C_3H_8 to Co^+. Using the technique of threshold collisional activation,[15] they obtained BDEs of 21.4 ± 1.2, 24.0 ± 0.7, and 30.9 ± 1.4 kcal/mol, respectively. These complexation energies are significantly larger than what was anticipated but appear to be consistent with a growing body of work on transition-metal–alkane clusters.[15,16] The importance of these results is that they support the notion that the reason transition-metal cations are particularly good at activating alkane C–H and C–C bonds is that the deep wells of the molecular complexes provide the reactants with enough internal energy to overcome the barriers to insertion and elimination—an advantage not possessed by neutral metal atoms.[17] This idea is further strengthened by the observation of an increasing complexation energy with the size of the alkane which correlates with increasing reactivity.[2,4-6]

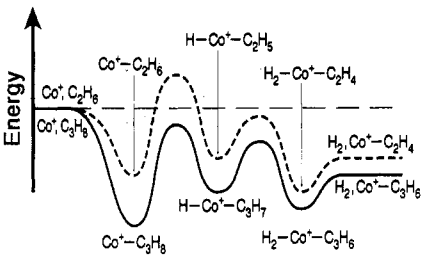

Figure 1. Schematic potential energy surfaces for Co^+-mediated elimination of H_2 from C_2H_6 (dashed line) and C_3H_8 (solid line). The deep well for the molecular complex of $Co(C_3H_8)^+$ leads to a barrier to insertion into a C–H bond which lies below the dissociation threshold. The more shallow well of $Co(C_2H_6)^+$ leads to a barrier which lies above this threshold, hence barring reaction.

Recent theoretical work by Bauschlicher, Partridge, and Langhoff[18] confirmed the large bond energy of Co^+ with H_2, obtaining a D_e of 17.3 kcal/mol. This is in contrast with CrH_2^+ (with a theoretical D_e of 7.0 kcal/mol) and NaH_2^+ (with a D_e of 3.1 kcal/mol). They attributed the stronger bond of Co^+ to more extensive sd hybridization and charge transfer. Importantly, the CoH_2^+ moiety was found to be a molecular complex—the H–H bond is not broken upon coordination to the Co^+.

Additional theoretical studies of transition-metal complexes with H_2 are abundant.[19-25] Most notable is the work of Balasubramanian,[19-22] who has looked extensively at the chemistry

* Author to whom correspondence should be addressed.
† California Institute of Technology.
‡ Ecole Polytechnique.
§ Contribution No. 8760.

0022-3654/93/2097-5238$04.00/0

of the second- and third-row transition metals. He has found large variations in geometries, with a number of metals inserting into the H–H bond to form large angle minima. In some cases, a barrier to insertion exists; in others there is none.

While much has been said on the bonding of molecular hydrogen to transition metals, considerably less has been said on the bonding of alkanes. Rosi et al.[26] looked at complexation of ethane to several transition-metal cations (Cu^+, Ag^+, Cr^+, and Mo^+) in their study of the dimethyl complexes of the first- and second-row transition metals. They identified two coordination sites: one possessing C_2 symmetry (favored by Cu^+) and one in which the metal is coordinated to two C–H bonds in C_s symmetry (favored by Ag^+). Berthier et al.[27] studied the complexation of CH_4 to Cu^+, and Hill, Freiser, and Bauschlicher[16] looked at the bonding of Cu^+, Y^{2+}, and Sc^{2+} to a number of hydrocarbons. In both of these studies, Cu^+ was found to coordinate to CH_4 in a C_{3v} geometry.

In this work, we present the results of high-level ab initio calculations on $Co(H_2)^+$, $Co(CH_4)^+$, $Co(C_2H_6)^+$, $Co(C_3H_8)^+$, and $Co(CH_4)_2^+$. In each case, a number of geometries and electronic states were investigated thoroughly. A detailed analysis of the nature of each bond is presented. The results of these calculations were used by Kemper et al.[13] to refine the analysis of their experimental data.

Computational Details

Our calculations used the modified coupled pair functional (MCPF) method,[28] a size-consistent modification of the HFSD configuration interaction (which includes all single and double excitations from the restricted Hartree–Fock wave function). This was the method of correlation used by Bauschlicher et al.[18] in their study of $Co(H_2)^+$, and it has been demonstrated to do quite well with electrostatic type bonds. Its primary advantages are that it is based on a single reference and that it is approximately size consistent, meaning that the treatment of $Co(H_2)^+$ and $Co(C_3H_8)^+$ should be of comparable quality. To better gauge the effectiveness of the method for this class of molecules, we provide a comparison with large (and time-consuming) multireference configuration interaction (MRCI) calculations for $Co(H_2)^+$. Test calculations using the more traditional HFSD method led to reasonable results for $Co(H_2)^+$ when the Davidson correction was included, but these calculations tended to underestimate the well depths for the larger alkanes by 2–3 kcal/mol (or ~10% of the bond energy) in comparison to the MCPF results.

The geometry of $Co(H_2)^+$ was fully optimized at the HF, MCPF, and MRCI levels under the constraint of C_{2v} symmetry. For the other complexes, a number of orientations of the metal to the alkane were considered at the MCPF level only (see Figure 2). It was expected that the alkane geometries would not change dramatically upon complexation to the metal. Hence the alkane was held fixed in its gas-phase experimental geometry, and only the metal–alkane distance was optimized at the MCPF level (in the case of $Co(C_2H_6)^+$ (η^3) C_s, this involved optimization of two degrees of freedom). A full gradient geometry optimization at the HF level leads to a metal–alkane distance which is too long, and hence an MCPF calculation done at this geometry underestimates the well depth by a few kilocalories per mole. On the other hand, we found that constraining the geometry of the alkane to remain at the free molecule structure in the MCPF optimization also tends to underestimate the complexation energy by a few kilocalories per mole. To account for the relaxation of the alkane geometry, we first carried out an MCPF minimization with fixed *alkane coordinates* and followed this with an HF gradient geometry optimization in which the *metal–alkane distance* was fixed to the MCPF optimum. The MCPF energy was then recomputed at this new geometry.

The vibrational frequency of the Co–alkane stretch was computed by fitting a cubic polynomial to four points about the minimum (at increments of 0.1 Å) and treating the system as a diatomic. This was based on data from the MCPF optimization and did not include the relaxation of the alkane. As a result, we expect these frequencies to be underestimated by ~10%. In the case of $Co(H_2)^+$, the H–H stretch was computed in a similar fashion, but the frequencies for this complex are expected to be more accurate, as a full geometry optimization was done. In the case of $Co(C_2H_6)^+$ (η^3) C_s, no frequencies were computed. From these data, it was possible to calculate approximate zero-point corrections for the bond energy. To roughly account for contributions from other modes (such as hindered rotations), we scaled the Co–alkane stretching frequency by a factor of 1.5.

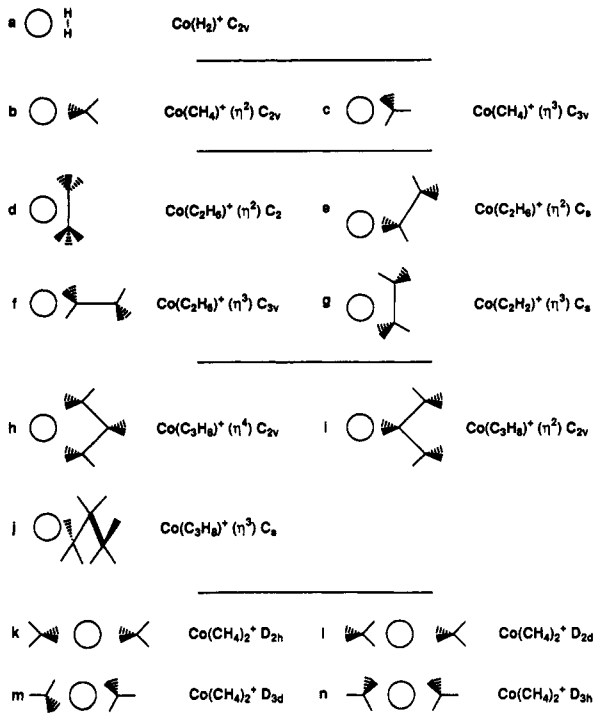

Figure 2. Geometries of the molecular complexes considered in this work: (a) $Co(H_2)^+$, (b, c) $Co(CH_4)^+$, (d–g) $Co(C_2H_6)^+$, (h–j) $Co(C_3H_8)^+$, and (k–n) $Co(CH_4)_2^+$.

We also made estimates of the contribution to the bond energy from the charge-induced polarization. This quantity was determined from $E_\alpha = -{}^1/_2\alpha q r_\alpha^{-4}$. The average polarizability, α, was taken from the literature; the charge on the ion, q, was taken as +1.0 esu; and the value of r_α was determined as $r_\alpha = (1/n)\sum_{i=1}^{n} r_A^{-4})^4$, where the r_A are the distances from the ion to all n atoms in the ligand. Determining r_α in such a manner takes into account the fact that the gradient of the electric field is quite large across the neutral molecule.

For Co, we used the relativistic effective core potential (RECP) of Christiansen, Ermler, and co-workers[29] and a triple-ζ quality basis set published elsewhere.[30] To this basis set we added two f polarization functions (exponents of 2.05 and 0.45). The tight function was optimized for the energy of the ^3F (d^8) ground state of Co^+ at the HFSD level, while the diffuse function was optimized for the ground state of CoH^+ at the generalized valence bond (GVB) level. We used the Huzinaga [11s7p] basis set for C contracted to (5s3p).[31] To this, two d polarization functions were added (exponents of 0.75 and 0.08), with the more diffuse function optimized for the polarizability of CH_4.[32] For H, we used the Dunning (6s/3s) basis set[33] and added two p polarization functions in the case of H_2 (exponents of 1.50 and 0.40), but only one in the larger alkanes (exponent of 1.00). During the HF-constrained geometry optimization, the Co f functions were removed from the basis set. In the case of $Co(C_3H_8)^+$, the carbon polarization functions were also removed. Removing these functions from this stage of the calculation should have minimal effect on the final MCPF energy.

Basis set superposition error calculations indicated that we overestimate the metal–ligand bond strengths by ~2 kcal/mol. This is due primarily to a deficiency in the ligand basis set. However, our experience suggests that this BSSE is more than compensated by basis set incompleteness. Improvements to the ligand basis set would lead to a better description of the polarizability and thus a stronger bond. Factoring in other sources of error such as the limitations in the method of correlation and the geometry optimization, we estimate that we *underestimate* bond strengths by 2 ± 1 kcal/mol.

All calculations used the MOLECULE/SWEDEN[34] and GVB[35] suites of programs on Alliant FX80/8 and FPS 522 computers.

Results and Discussion

$Co(H_2)^+$. The ground state of $Co(H_2)^+$ has the metal in its ground-state configuration [^3F (d^8)]. With C_{2v} symmetry (see Figure 2a), the attraction to Co^+ is electrostatic in origin and the H_2 retains its bonding character (the H–H bond length increases only 0.06 Å—from 0.74 to 0.80 Å). Insertion is found to be an endothermic process, and no stable dihydride can be formed. Numerous examples of dihydrogen molecular complexes with transition-metal cations have been documented by theoretical chemists,[18-22,25] and the first organometallic compounds containing such ligands were found in 1984 [$M(CO)_3(PR_3)_2(H_2)$, (M = Mo, W; R = Cy, *i*-Pr)].[36] For $Co(H_2)^+$, at the highest level of calculation (MRCI + Q, defined below), we find a bond dissociation energy of D_e = 18.3 kcal/mol ($D_0°$ ~ 16.4 kcal/mol) compared to the experimental value of $D_0°$ = 18.2 ± 1.0 kcal/mol.[12] These numbers also compare well to the recent MCPF results of D_e = 17.3 kcal/mol.[18]

The formation of the $Co(H_2)^+$ bond involves a number of factors. These are primarily (i) charge-induced dipole interactions, (ii) charge–quadrupole interactions, (iii) polarization of charge on the metal, and (iv) charge transfer. The bond is dominated by the charge-induced dipole interaction, which contributes an estimated 15.9 kcal/mol to the well depth (r_α = 1.70 Å and α = 0.80 Å^3).[37] The charge–quadrupole interaction contributes another 5.0 kcal/mol. It is believed that the polarization of charge on the metal and charge transfer serve to reduce Pauli repulsion and shorten the bond length. As both of these factors depend on a well-correlated wave function, a considerable change in the geometry is observed in going from the HF to the CI level (the Co–H_2 bond length shortens by 0.3 Å). Consequently, the electrostatic contributions increase since the charge-induced polarization is proportional to r^{-4} and the charge–quadrupole is proportional to r^{-3}. The CI well depth is thus more than twice the HF well depth.

Charge transfer (see Figure 3a,b) follows the Dewar–Chatt model for bonding to alkenes and alkynes. The H_2 bond ($1\sigma_g$) acts as a two-electron donor and lends charge to the empty 4s orbital of the Co^+ (Figure 3a). There is also some back-bonding involving charge transfer from the doubly occupied Co^+ $3d_{yz}$ orbital to the empty H_2 antibonding orbital ($1\sigma_u$) (as in Figure 3b, note the molecule is in the *yz* plane with *z* the principal axis). The Mulliken populations and the direction of the dipole moment indicate that charge transfer from H_2 to the metal dominates. This σ-donor–π-acceptor nature of the bond is also evident in the decrease in the H–H stretch from 44[illegible] cm^{-1} for free H_2 (4404 cm^{-1} experimentally[38]) to 3580 cm^{-1} upon complexation.

The eight metal valence electrons are distributed as follows:

$$(b_2\, d_{yz})^2(b_1\, d_{xz})^2(a_1\, d_{x^2-y^2})^2(a_1\, d_{z^2})^1(a_2\, d_{xy})^1$$

leading to a $^3A_2$ ground state. The d_{z^2} orbital is singly occupied because of the repulsive interaction with the H_2 bonding orbital ($1\sigma_g$). The d_{xy} is thus singly occupied in order to maintain the ^3F character of the Co^+. The $^3A_1$ state ($d_{x^2-y^2}$ to d_{xy} excitation) is nearly degenerate (0.1 kcal/mol above the ground state), and the $^3B_1$ state (d_{xz} to d_{xy} excitation) is 4.7 kcal/mol higher. The $^3A_1$ state is similar in character to the ground state, but other configurations ($^3B_1$ and $^3B_2$) introduce the higher energy ^3P state on the metal, compromise the Co–H_2 charge transfer, or increase repulsion to the H_2 bonding orbital ($1\sigma_g$). In addition, the first excited state of Co^+, ^5F (s^1d^7), forms only a weak molecular complex as the occupied 4s orbital is repulsive to the H_2, resulting in a longer Co–H_2 bond and reduced electrostatic interactions. The linear Co–H_2 geometry is only weakly bound as well.

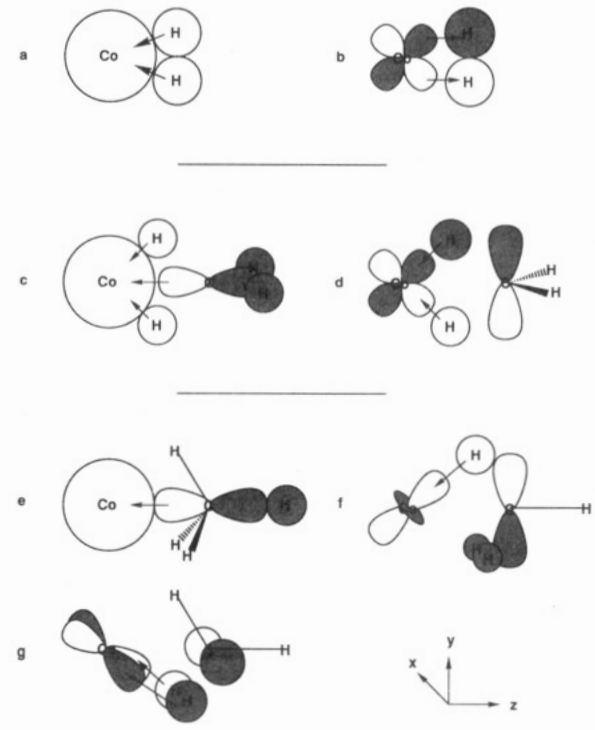

Figure 3. Charge-transfer schematic for various Co^+–ligand bonds: (a, b) $Co(H_2)^+$, showing donation into the Co^+ 4s and back-donation from the Co^+ $3d_{yz}$. (c, d) η^2 $Co(CH_4)^+$, showing donation into the Co^+ 4s and $3d_{yz}$. (e–g) η^3 $Co(CH_4)^+$, showing donation into the Co^+ 4s, $3d_\sigma$, and $3d_\delta$.

TABLE I: Configurations Used as References in the MRCI Calculation for $Co(H_2)^+$ [a]

$3a_1$ Co $d_{x^2-y^2}$	$2b_1$ Co d_{xz}	$5a_1$ Co d_{z^2}	$1a_2$ Co d_{xy}	$4a_1$ H_2 σ_g	$2b_2$ Co d_{yz}	$3b_2$ H_2 σ_u	$6a_1$ Co 4s
2	2	1	1	2	2	0	0
2	2	1	1	2	0	2	0
2	2	1	1	0	2	2	0
2	2	1	1	0	2	0	2
2	2	1	1	1	1	1	1
2	2	1	1	2	1	1	0
2	2	1	1	1	2	0	1

[a] The inactive core orbitals include the a_1 Co 3s and $3p_z$, the b_1 Co $3p_x$, and the b_2 Co $3p_y$.

Calculations on the ground state were also performed at the MCPF level. The results (D_e = 17.2 kcal/mol) are nearly identical to those of Bauschlicher et al.,[18] as the calculations differ only in the choice of basis set and the use of the effective core potential. The accuracy of this method is tested by comparison with the more conventional MRCI technique. The MRCI is based on a CASSCF wave function in which six electrons are correlated in six orbitals (including the two H_2 bonding electrons, the two Co^+ d_{yz} back-bonding electrons, and the two open-shell electrons). This corresponds to the GVB-CI(6/6) wave function. The MRCI is specified by choosing seven reference configurations from this CASSCF and including all single and double excitations into the virtual space from all seven configurations. Table I lists the reference configurations for the MRCI, and the results are summarized in Table II. Overall, the MCPF method fares quite

TABLE II: Comparison of HF, MCPF, and MRCI + Q Results for $Co(H_2)^+$

	HF	MCPF	MRCI + Q
D_e (kcal/mol)[a]	8.1	17.2	18.3[b]
r_e (Co—H_2, Å)	1.94	1.69	1.66
r_e (H—H, Å)	0.75	0.79	0.80
ω_e (Co—H_2, cm^{-1})	560	902	909
ω_e (H—H, cm^{-1})	4340	3710	3580
μ (D)[c]	+0.714	+0.323	+0.384
charge on Co	+0.856	+0.768	+0.780

[a] The experimental value is $D_0° = 18.2 \pm 1.0$ kcal/mol.[12] The zero-point correction is estimated to be 1.9 kcal/mol. [b] The MRCI bond energy without the inclusion of the Davidson correction (designated +Q) is 16.9 kcal/mol. The HFSD energy is 14.6 kcal/mol. The HFSD + Q energy is 16.8 kcal/mol. [c] The dipole moment is calculated with the Co^+ at the origin. The positive sign suggests charge transfer from the H_2 to the Co^+.

TABLE III: Properties of $Co(CH_4)^+$

	η^2 C_{2v}	η^3 C_{3v}		η^2 C_{2v}	η^3 C_{3v}
D_e (kcal/mol)[a]	21.4	20.1	E_α (kcal/mol)[b]	17.7	18.2
D_e (unrelaxed)	19.5	19.0	r_α (Å)[c]	2.22	2.20
ω_e (Co—C, cm^{-1})	343	340	μ (D)	+2.178	+2.354
r_e (Co—C, Å)	2.24	2.11	charge on Co	+0.655	+0.684
r_e (Co—H, Å)	1.94	2.11			

[a] The experimental values are $D_0° = 22.9 \pm 0.7$[13] and 21.4 ± 1.2 kcal/mol.[14] The zero-point correction is estimated to be 0.7 kcal/mol. [b] Contribution to the energy from the charge-induced dipole. [c] r_α is used to compute the charge-induced dipole. See text.

well. Indeed, MCPF appears to do slightly better than MRCI without the Davidson correction. MRCI *with* the Davidson correction compared to MCPF leads to a slightly stronger Co^+–H_2 bond (D_e = 18.3 vs 17.2 kcal/mol), a slightly shorter Co–H_2 distance (1.66 vs 1.69 Å), and a weaker H–H bond upon complexation (ν_{H-H} = 3580 vs 3710 cm^{-1}). However, the number of MRCI spin eigenfunctions is quite large compared to that of MCPF (378 211 vs 12 592), leading to prohibitively large calculations for the complexes with CH_4, C_2H_6, and C_3H_8. Since electron correlation is essential (HF accounts for only 44% of the bond energy) and size consistency is desired, MCPF is the method of choice for describing the complexation of the larger molecules to Co^+.

$Co(CH_4)^+$. The results for the complexation of CH_4 to Co^+ are given in Table III. We find D_e = 21.4 kcal/mol ($D_0° \sim 20.7$ kcal/mol), in excellent agreement with the experimental values of $D_0° = 22.9 \pm 0.7$[13] and 21.4 ± 1.2 kcal/mol.[14] However, in contrast to previous theoretical findings that $Cu(CH_4)^+$ has an η^3 C_{3v} structure (Figure 2c), we find the η^2 C_{2v} geometry (Figure 2b) to be more stable. This geometry is not without precedent. It has been identified as a precursor to insertion into a methane C–H bond (oxidative addition) by both bare[39,40] and ligated metals.[41,42] The geometry is also consistent with the η^2 C_s geometry of $Ag(C_2H_6)^+$ found by Rosi et al.[26] The difference in energy between the η^2 C_{2v} and η^3 C_{3v} structures of $Co(CH_4)^+$ is only 1.3 kcal/mol (the η^1 structure is worth <12 kcal/mol), and the advantages in forming an η^2 complex are subtle. We find these advantages to be reduction in Pauli repulsion and increased charge transfer.

The ground state of the η^2 C_{2v} complex has a Co^+ configuration of

$$(a_1\ d_{y^2-z^2})^2(a_2\ d_{xy})^2(b_1\ d_{xz})^2(a_1\ d_{x^2})^1(b_2\ d_{yz})^1$$

where the two C–H bonds coordinated to the Co^+ are in the yz plane and z is the principal axis. This leads to a $^3B_2$ state. Careful analysis of the $Co(CH_4)^+$ MCPF natural orbitals (including a study of the Mulliken populations and the dipole moments) suggests that there is charge transfer from the CH_4 to the metal from both the a_1 and b_2 symmetries with no evidence of back-bonding. While H_2 is a two-electron donor (with some π acid character), η^2-CH_4 is a *four*-electron donor. This is illustrated in parts c and d of Figure 3. The two C–H bonds coordinated to the metal transform under the a_1 and b_2 irreducible representations, and it is these orbitals which donate charge to the metal. As expected, charge transfer is dominantly from the CH_4 $3a_1$ orbital into the empty Co^+ a_1 4s orbital. The charge transfer in b_2 symmetry is significantly smaller, but the Co^+ b_2 d_{yz} orbital is singly rather than doubly occupied in order to accommodate the increased charge. The dominant effect of having this orbital singly occupied, however, is to reduce Pauli repulsion to the C–H bonds. As in $Co(H_2)^+$, since the d_{yz} orbital is singly occupied, the d_{x^2} orbital is singly occupied in order to maintain the ^3F character of the metal. Among the nonbonding orbitals, the $d_{y^2-z^2}$ is found to hybridize extensively with the 4s. The d orbital is thus polarized along the y axis, reducing its repulsion to the ligand along the z direction. Blomberg et al. noted that this hybridization has the effect of deshielding the metal nucleus from the methane, thereby increasing the electrostatic components of the bond.[40] It also leaves the empty 4s orbital polarized along the z axis, increasing the metal's ability to accept charge from the ligand. Upon insertion into a C–H bond from this state, increasing back-donation from the $d_{y^2-z^2}$ orbital should be observed.

One might have expected the a_1 d_{z^2} orbital to be the most repulsive to the methane and, thus, the most likely to be singly occupied. Hence, we also considered in detail the $^3A_2$ state with the Co^+ configuration:

$$(b_2\ d_{yz})^2(b_1\ d_{xz})^2(a_1\ d_{x^2-y^2})^2(a_1\ d_{z^2})^1(a_2\ d_{xy})^1$$

In this state, the a_2 d_{xy} orbital is also singly occupied, as in the ground state of $Co(H_2)^+$. The bond was found to be worth 18.0 kcal/mol (16.8 kcal/mol without relaxation of the methane geometry), which is 3.4 kcal/mol weaker than the $^3B_2$ ground state. Additionally, the Co–C distance is ~0.1 Å longer (2.36 Å) and the Co–CH_4 stretch is smaller (314 cm^{-1}) than for the $^3B_2$ state. While charge donation occurs from the CH_4 $3a_1$ orbital into the Co 4s, the a_2 d_{xy} orbital is not suitable for accepting charge and does little to reduce Pauli repulsion to the ligand. The s-d hybridization is smaller in this state, and there is no evidence for back-bonding similar to that of $Co(H_2)^+$. This is surely responsible for the weaker bond.

For the η^3 C_{3v} structure, a similar situation exists. In this case, the methane is a *six*-electron donor with the three C–H bonds transforming under the a_1, e(a′), and e(a″) symmetries. The behavior of the Co^+ as an acceptor is, however, somewhat unusual. Again, with z the principal axis, the d_{z^2} orbital is doubly occupied and hybridizes with the empty 4s to reduce repulsion and polarize the charge-accepting 4s orbital in the z direction. The additional metal orbitals are linear combinations of the d_π and d_δ orbitals, such that the two that are singly occupied possess approximately σ and δ character offset from the z axis by an angle of 54.74°. This magic angle produces a d_σ orbital from $(^2/_3)^{1/2}yz + (^1/_3)^{1/2}(x^2 - y^2)$ and a d_δ orbital with respect to this of $(^2/_3)^{1/2}xz - (^1/_3)^{1/2}xy$. The σ–δ character of the singly occupied orbitals ensures that the metal is in its ^3F state and most effectively reduces Pauli repulsion to the ligand. It also allows for charge transfer as indicated in Figure 3e–g. As expected, this charge transfer occurs from the CH_4 $3a_1$ orbital into the metal 4s (hybridized with the d_{z^2}), as in Figure 3e. In addition, charge is donated into the two singly occupied orbitals of the metal: from the CH_4 e(a′) into the σ-like orbital (Figure 3f) and from the CH_4 e(a″) into the δ-like orbital (Figure 3g). In sum, η^3-CH_4 is like a tridentate ligand coordinated facially to the Co^+.

It should be emphasized that the strength of the Co^+–CH_4 bond is primarily due to charge-induced polarization. However, estimates of the contribution to the bond energy from this effect suggest that the η^3 conformation should be slightly stronger than the η^2 conformation (18.2 vs 17.7 kcal/mol). Consideration of other factors, such as Pauli repulsion, charge transfer from the CH_4 to the Co^+, and polarization of the nonbonding orbitals on

TABLE IV: Properties of $Co(C_2H_6)^+$

	η^3 C_s	η^2 C_2	η^2 C_s	η^3 C_{3v}
D_e (kcal/mol)[a]	25.0	24.9	24.7	23.6
D_e (unrelaxed)	23.6	22.8	22.6	22.4
ω_e (Co—C, cm^{-1})	–	261	286	288
r_e (Co—C, Å)	2.14, 2.45[b]	2.34 (2.21)[c]	2.23	2.09
r_e (Co—H, Å)	2.05, 2.04[d]	1.96	1.90	2.05
E_α (kcal/mol)	25.5	23.8	21.3	22.1
r_α, (Å)	2.32	2.36	2.43	2.40
μ (D)	+3.037	+2.923	+2.890	+3.327
charge on Co	+0.612	+0.665	+0.623	+0.632

[a] The experimental values are $D_0° = 28.0 \bullet 1.1$[13] and 24.0 ± 0.7 kcal/mol.[14] The zero-point correction is estimated to be 0.6 kcal/mol. [b] Distances to both carbons are given. The first (C_1) has two C—H bonds coordinated to the metal, and the second (C_2) has only one. [c] The number in parentheses is the distance from the Co to the C—C bond midpoint. [d] The first number is the distance to the two H atoms bound to C_1 which are coordinated to the metal, and the second is the distance to the H bound to C_2 which is coordinated to the metal.

the metal, leads to a reversal of order for these two states. That is, charge transfer and s–d hybridization appear to be less effective in η^3 $Co(CH_4)^+$ than in η^2 $Co(CH_4)^+$, resulting in a weaker bond. Comparison with results for $Cu(CH_4)^+$ demonstrates how the presence of open-shell d electrons and a low-lying empty 4s orbital on Co^+ increase the effectiveness of these two contributions to the bonding. Cu^+, with a d^{10} ground state and a high-energy 4s orbital, leads to a C_{3v} ground state for $Cu(CH_4)^+$ with a bond energy of only 14.8 kcal/mol (MCPF)[16] (18.1 kcal/mol (MP2)[27]).

Finally, the changes in the geometry of the CH_4 in the η^2 complex from its free structure should be noted. There is an increase in the bond lengths (0.016 Å) and angle (10.3°) of the two C–H bonds coordinated to the metal. The two bonds directed away from the metal show little change. The effect of this relaxation is to lower the energy of the complex by 2.9 kcal/mol with respect to the separated metal and methane. The C_{3v} complex shows less of a change in the CH_4 geometry, adding only 1.1 kcal/mol to the bond strength.

$Co(C_2H_6)^+$. The potential energy surface for $Co(C_2H_6)^+$ is quite flat. Four different coordination sites (Figure 2d–g) were investigated, with the difference in BDEs being ≤1.4 kcal/mol (see Table IV). The strongest bond involves coordination of Co^+ to two carbon centers under C_s symmetry (Figure 2g). The complexation energy is $D_e = 25.0$ kcal/mol ($D_0° \sim 24.4$ kcal/mol), compared to the experimental values of $D_0° = 28.0 \pm 1.1$[13] and $D_0° = 24.0 \pm 0.7$[14] kcal/mol. Nearly degenerate, the C_2 structure (also involving coordination to two carbon centers, see Figure 2d) is only 0.1 kcal/mol higher in energy ($D_e = 24.9$ kcal/mol, $D_0° \sim 24.3$ kcal/mol). The η^2 C_s structure, which has Co^+ coordinated to two C–H bonds on the same carbon center (see Figure 2e), is 0.3 kcal/mol higher than the lowest energy structure ($D_e = 24.7$ kcal/mol, $D_0° \sim 24.1$ kcal/mol), and the η^3 C_{3v} structure (coordination to three C–H bonds on the same carbon center, see Figure 2f) is 1.4 kcal/mol higher ($D_e = 23.6$ kcal/mol, $D_0° \sim 23.0$ kcal/mol). The splitting between the energies of the three lowest states is certainly within the error bars of the calculations, so a definitive statement as to the ground-state geometry cannot be made.

While it would appear that the C_2 and C_s geometries of $Co(C_2H_6)^+$ (which describe coordination of Co^+ to two carbons) are comparable to that of $Co(H_2)^+$ (i.e., coordination to the C–C or H–H bond), the bonding is more consistently described as η^2 or η^3 coordination of the metal to one C–H bond on one carbon and one C–H bond (η^2 C_2 geometry) or two C–H bonds (η^3 C_s geometry) on the other. We conclude this because the Co–H distances are comparable to those in $Co(CH_4)^+$. In addition, the Co^+ is approximately equidistant from the three hydrogens in the η^3 C_s geometry of $Co(C_2H_6)^+$ but is significantly closer to one of the carbons than the other (r_e(Co–C) = 2.14 and 2.45 Å). The η^3 C_s configuration of $Co(C_2H_6)^+$ is also consistent with our arguments for bonding in η^3 $Co(CH_4)^+$. There is a singly occupied d_σ-like orbital directed toward the in-plane C–H bond and a singly occupied d_δ-like orbital directed toward the two out-of-plane C–H bonds on the other carbon. Both of these orbitals accept charge from the ethane, as does the 4s orbital. The η^2 C_2 state is consistent with our arguments for charge transfer from two C–H bonds in η^2 $Co(CH_4)^+$ as well. That is, a d_π orbital, approximately in the H–Co–H plane, is singly occupied and accepts charge from the ligand. In contrast, Co^+ strictly coordinating to the C–C bond would likely possess d_{z^2} and d_{xy} holes (with the C–Co–C backbone in the yz plane and z the C_2 axis of rotation), as in the ground state of $Co(H_2)^+$. Such a state would have a doubly occupied d_{yz} orbital capable of back-bonding to the C–C bond, resulting in a molecular complex suitable for insertion into the C–C bond.

The η^2 coordination of two C–H bonds on the *same* carbon center (C_s symmetry, see Figure 2e) is only 0.3 kcal/mol higher in energy than the lowest energy η^3 C_s state and only 0.2 kcal/mol higher in energy than the η^2 C_2 state. It shows the same characteristics of η^2 coordination as for the C_{2v} structure of $Co(CH_4)^+$ and, indeed, the C_2 structure of $Co(C_2H_6)^+$. Strong similarities between the nature of these two conformations of $Co(C_2H_6)^+$ can be seen. The Co–H distance is only slightly shorter in the C_s geometry (1.90 Å) than in the C_2 geometry (1.96 Å), and relaxation of the C_s ethane geometry contributes 2.1 kcal/mol to the bond energy in both structures. In addition, the coordinated C–H bond lengths increase in both geometries by 0.02 Å upon complexation to the metal ($R_{C-H} = 1.105$ Å for the C_2 structure and $R_{C-H} = 1.107$ Å for the C_s structure). Clearly, the similarity between these two structures suggests that η^2 *coordination to C–H bonds is favorable for Co^+ regardless of whether the bonds are on the same center or different centers.*

The η^3 coordination to a single carbon of C_2H_6 in C_{3v} symmetry (Figure 2f) is worth 23.6 kcal/mol. This is higher in energy than the ground-state η^3 C_s structure by 1.4 kcal/mol. The nature of the bond is entirely analogous to that of C_{3v} $Co(CH_4)^+$. There are, however, a number of additional advantages for $Co(C_2H_6)^+$. Namely, this geometry is consistent with coordination to the negative quadrupole moment of C_2H_6, and it can take the most advantage of the polarizability of the C–C bond.

The observation that the low-lying states are more characteristic of precursors to insertion into C–H bonds rather than the C–C bond is consistent with kinetic data.[6] Isotope labeling experiments on $Co(C_3H_8)^+$ suggest that the initial, rate-determining step in the elimination of CH_4 and H_2 from C_3H_8 is insertion into a C–H bond. The *second* step involves insertion into either a C–H bond (H_2 elimination) or a C–C bond (CH_4 elimination). The theoretical work of Low and Goddard[39,43] on the oxidative addition of H_2, CH_4, and C_2H_6 to Pd and Pt complexes shows that the barrier is much greater for insertion into the C–C bond than for insertion into a C–H bond; however, our results underscore a bias toward C–H bond activation present even in the molecular complexes.

Finally, the increased bond strength of $Co(C_2H_6)^+$ as compared to that of $Co(CH_4)^+$ is principally due to an increase in the polarizability of the ligand ($\alpha(CH_4) = 2.59$ Å^3, $\alpha(C_2H_6) = 4.47$ Å^3).[37] The relationship is clearly not linear, however, reflecting the fact that the increasing size of the ligand increases the value of r_α. We calculate the contribution from charge-induced polarization in $Co(C_2H_6)^+$ to range from 21.3 kcal/mol (for the η^2 C_s structure) to 25.5 kcal/mol (for the η^3 C_s structure). Evidence for the importance of polarizability on the bond strength is seen in the large increase in the dipole moment in going from $Co(CH_4)^+$ to $Co(C_2H_6)^+$. A decrease in the ionization potential of the ligand ($IP(CH_4) = 12.70$ eV, $IP(C_2H_6) = 11.52$ eV)[44] may facilitate increased charge transfer (the charge on the metal is in fact smaller for $Co(C_2H_6)^+$ than for $Co(CH_4)^+$), also affecting the bond length and bond strength.

$Co(C_3H_8)^+$. Due to the size of the $Co(C_3H_8)^+$ calculations,

TABLE V: Properties of $Co(C_3H_8)^+$

	η^4 C_{2v}	η^2 C_{2v}		η^4 C_{2v}	η^2 C_{2v}
D_e (kcal/mol)[a]	27.6	26.8	E_α (kcal/mol)	25.9	23.3
D_e (unrelaxed)	26.3	25.0	r_α (Å)	2.52	2.59
ω_e (Co—C,cm^{-1})	220	256	μ (D)	+3.515	+3.342
r_e (Co—C, Å)[b]	2.41 (2.89)	2.23	charge on Co	+0.699	+0.608
r_e (Co—H, Å)	2.19	1.89			

[a] The experimental value is $D_0° = 30.9 \pm 1.4$ kcal/mol.[14] The zero-point correction is estimated to be 0.5 kcal/mol. [b] r_e is the distance from the Co to the nearest carbon. For the η^4 case, the distance to the secondary carbon is given in parentheses.

we considered only the two most likely high-symmetry coordination sites in detail. These are the η^2 coordination to the secondary carbon (Figure 2i) and the η^4 coordination to the two primary carbons (Figure 2h), both with C_{2v} symmetry. Other possible sites, including η^2 and η^3 coordinations to a primary carbon or η^2 and η^3 coordination to a primary and secondary carbon, have lower symmetry structures (C_s or C_1) and have not yet been calculated. We estimate that these structures could be 1–2 kcal/mol more stable than the high-symmetry conformations.

As detailed in Table V, we find the η^4 geometry to be lower in energy than the η^2 geometry by 0.8 kcal/mol out of 27.6 kcal/mol ($D_0° \sim 27.1$ kcal/mol). This is somewhat shy of the experimental value of $D_0° = 30.9 \pm 1.4$ kcal/mol.[14] While the η^2 structure shows the same characteristics as $Co(CH_4)^+$ and $Co(C_2H_6)^+$, the η^4 structure is somewhat different. It still appears to be more appropriately described as coordination to four C–H bonds rather than coordination to the carbons. The ground state has a Co^+ configuration of

$$(a_1\, d_{y^2-z^2})^2(a_2\, d_{xy})^2(b_1\, d_{xz})^2(a_1\, d_{x^2})^1(b_2\, d_{yz})^1$$

The Co and the C–C–C backbone are in the yz plane, and z is the principal axis. The singly occupied d_{yz} orbital minimizes repulsion to the ligand. However, the Co–H distance is 2.19 Å compared to 1.89 Å for the η^2 structure, the C–H bond lengthening is about 0.01 Å smaller than in the η^2 geometry, and less charge is transferred to the metal than in the η^2 structure. The finding that the η^4 conformation is more stable is probably a result of better charge-induced polarization, which we calculate to be 25.9 vs 23.3 kcal/mol for the η^2 structure.

On the basis of the results of the $Co(CH_4)^+$ and $Co(C_2H_6)^+$ calculations, we attempted a guess at the geometry of a third conformation. This geometry involves η^3 coordination of the Co^+ to all three carbons in C_s symmetry (see Figure 2j). The position of the Co^+ is such that it is 1.91 Å from each of the three hydrogens to which it is coordinated. The metal is then 2.25 Å from the secondary carbon and 2.45 Å from each of the primary carbons. Only a single point was calculated, and the propane geometry was not allowed to relax. The motivation for doing such a calculation came from the large estimate for the charge-induced polarization—34.9 kcal/mol. The magnitude of this number strongly suggested that this conformation is the ground state. Our calculations give a bond energy of 27.7 kcal/mol, 1.4 kcal/mol better than the unrelaxed D_e of the η^4 structure. Estimating the relaxation of the propane to contribute another 1.6 ± 0.4 kcal/mol (the mean relaxation energy calculated for $Co(CH_4)^+$, $Co(C_2H_6)^+$, and $Co(C_3H_8)^+$), $D_e = 29.3 \pm 0.4$ kcal/mol for the η^3 conformation.

The difference in energy between this cluster and that of $Co(C_2H_6)^+$ is quite small (4.3 kcal/mol theoretically, 6.9 kcal/mol experimentally[14]), yet their chemistry is markedly different. Falling back on the postulate put forth in the Introduction that the barrier for oxidative addition is relatively constant from alkane to alkane and considering that the barrier for insertion into a C–H bond of C_3H_8 lies only 3 kcal/mol below the dissociation threshold,[6] the barrier for insertion of Co^+ into a C–H bond of C_2H_6 therefore should lie only a few kcal/mol above the dissociation threshold.

TABLE VI: Properties of $Co(CH_4)_2^+$

	D_{2h}	D_{3d}	D_{2d}
D_e (kcal/mol)[a]	23.1	21.4	14.8
D_e (unrelaxed)	21.4	21.2	14.4
ω_e (sym C—Co—C, cm^{-1})	318	322	293
r_e (Co—C, Å)	2.23	2.09	2.34
r_e (Co—H, Å)	1.93	2.09	2.00
E_α (kcal/mol)[b]	18.3	20.0	13.3
r_α (Å)	2.21	2.19	2.30
charge on Co	+0.428	+0.480	+0.513

[a] The experimental values are $D_0° = 24.8 \pm 0.8$ kcal/mol[13] and 23.3 ± 1.2 kcal/mol.[14] The zero-point correction is estimated to be 0.7 kcal/mol. [b] E_α is given as the total contribution of charge-induced polarization to the energy of $Co(CH_4)_2^+ - 17.7$ kcal/mol (the contribution of charge-induced polarization to the energy of C_{2v} $Co(CH_4)^+$).

$Co(CH_4)_2^+$. Kemper, Bowers, and co-workers[13] also examined experimentally the complexation of multiple ligands to Co^+. In support of this work, we looked at the complexation of a second methane to $Co(CH_4)^+$, and the results are given in Table VI. In agreement with experiment, the complexation energy of the second methane is *larger* than that of the first. We find $D_e = 23.1$ kcal/mol ($D_0° \sim 22.4$ kcal/mol vs $D_0° \sim 20.7$ kcal/mol for the first Co^+–CH_4 bond), compared to the experimental value of $D_0° = 24.8 \pm 0.8$ kcal/mol (vs 22.9 ± 0.7 kcal/mol for the first bond).[13] This is also in agreement with the results of Haynes and Armentrout,[14] who obtained a second bond energy of $D_0° = 23.3 \pm 1.2$ vs 21.4 ± 1.2 kcal/mol for the first.

The ground state involves η^2 coordination of both methanes to the metal with a C–Co–C angle of 180°. Contrary to the results of Bauschlicher et al.[18] for $Co(H_2)_2^+$, in which the H_2 ligands were found to be *staggered* in a D_{2d} conformation, we find the four C–H bonds coordinated to the metal to be *eclipsed* in a D_{2h} geometry (Figure 2k). Moreover, the difference in energy between the D_{2h} and D_{2d} conformations (Figure 2l) is quite large for $Co(CH_4)_2^+$ (8.3 kcal/mol), compared to only 1.4 kcal/mol for D_{2d} $Co(H_2)_2^+$ vs the D_{2h} geometry.

When one considers that H_2 is a σ-donor–π-acceptor but CH_4 is a four-electron donor, the reasons for the marked difference between $Co(CH_4)_2^+$ and $Co(H_2)_2^+$ are quite clear. The bonding in the D_{2h} ground state of $Co(CH_4)_2^+$ is no different in concept from that of η^2 $Co(CH_4)^+$. The Co^+ configuration is still

$$(a_g\, d_{y^2-z^2})^2(b_{1g}\, d_{xy})^2(b_{2g}\, d_{xz})^2(a_g\, d_{x^2})^1(b_{3g}\, d_{yz})^1$$

Again, z is the principal axis, and the four C–H bonds coordinated to the metal are in the yz plane. This leads to a $^3B_{3g}$ ground state. The 4s (hybridized with the $d_{y^2-z^2}$) and the d_{yz} orbitals of Co^+ accept charge from the two methanes. This requires that the coordinating C–H bonds of both methanes be in the yz plane, leading to the eclipsed D_{2h} geometry of $Co(CH_4)_2^+$.

The lowest energy D_{2d} state has the d_{z^2} and d_{xy} (or $d_{x^2-y^2}$) orbitals singly occupied. The d_δ orbital is not of a symmetry appropriate for accepting charge from the ligands, and having it singly occupied does little to reduce Pauli repulsion. Thus, the advantages of bonding present in the D_{2h} geometry are lost, and the bond is much weaker. Charge is donated only into the Co 4s orbital.

In the case of $Co(H_2)_2^+$, there are no such biases favoring either the staggered (D_{2d}) or eclipsed (D_{2h}) geometries, either from the occupations of the Co orbitals (both d_π orbitals are doubly occupied) or from s-d hybridization. As argued by Bauschlicher et al.,[18] the staggered conformation is favored because it leads to back-bonding from two different metal d_π orbitals as opposed to back-bonding from the same orbital. More to the point, in the D_{2d} geometry, one d_π orbital is polarized toward the first H_2 molecule and the other d_π orbital is polarized toward the second. Still, this difference is subtle compared to the difference between the D_{2h} and D_{2d} configurations of $Co(CH_4)_2^+$, and the energy splitting between the two structures is small.

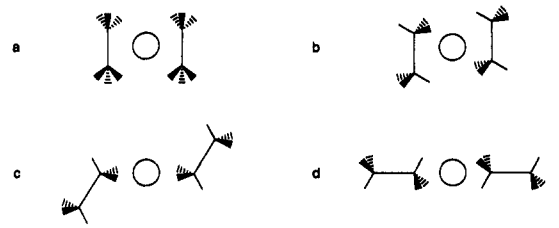

Figure 4. Possible geometries for $Co(C_2H_6)_2^+$. (a) and (c) have a square-planar arrangement of four C–H bonds about the metal. (b) and (d) have an octahedral arrangement of six C–H bonds about the metal.

As for the increase in the bond energy for the second methane, this is likely due to the hybridization of the $d_{y^2-z^2}$ and 4s orbitals. There is some cost in energy associated with this hybridization, and this is accounted for in the complexation of the first methane. As the hybridization is already appropriate for complexation of a second methane (in the D_{2h} geometry), the second bond energy is larger (suggesting that the energy cost of hybridization is at least 1.7 kcal/mol).

We have also examined coordination of a second methane in the η^3 conformation. In this case, we find the bonds to be *staggered* in a D_{3d} geometry (Figure 2m). The bond is worth 21.4 kcal/mol ($D_0° \sim 20.7$ kcal/mol) with respect to $CH_4 + C_{2v}$ $Co(CH_4)^+$, 1.7 kcal/mol higher than the D_{2h} ground state. The fact that the methanes are staggered is consistent with the description of the η^3 C_{3v} $Co(CH_4)^+$ bond as already detailed and pictured in Figure 3e–g. The singly occupied d_σ and d_δ orbitals (off the principal axis by 54.74°) lead to the greatest reduction in Pauli repulsion if the six coordinated C–H bonds are in an octahedral (albeit, trigonally distorted) arrangement (i.e., staggered).

Unfortunately, examination of the eclipsed η^3 (D_{3h}) geometry (Figure 2n) led to a breakdown in the MCPF method. This is because the lowest energy state in this geometry is not well described by a single configuration. It involves dominantly Co d_{xz} and d_{yz} (π–π) holes but with a large coefficient for the configuration having d_{xy} and $d_{x^2-y^2}$ (δ–δ) holes. The single occupation of the two π orbitals is the best overall configuration for reducing Pauli repulsion, but the incorporation of the second configuration is to preserve the ^3F character of the Co^+ (a state with pure π–π holes has a character which is 80% ^3F and 20% ^3P).[45] The MCPF method overcompensates and mixes in too much of the configuration with (δ–δ) holes. Test singles and doubles CI calculations based on one-configuration HF and on two-configuration MCSCF wave functions show this state to be 1.0 kcal/mol higher in energy than the D_{3d} (staggered) geometry.

Similar results may be expected for $Co(C_2H_6)_2^+$. The most likely structures are pictured in Figure 4. Kemper, Bowers, and co-workers[13] found the second bond to be slightly weaker than the first ($D_0° = 26.8 \pm 1.0$ vs 28.0 ± 1.6 kcal/mol). This may be due to steric effects, which would be greatest in the two structures shown in Figure 4a,b.

Conclusions

We used the MCPF method to consider the molecular complexation of H_2 and a number of small hydrocarbons (CH_4, a second CH_4, C_2H_6, and C_3H_8) with Co^+. Our results (which were done independently) compare quite well to the recent experimental work of Kemper, Bowers, and co-workers[12,13] and of Haynes and Armentrout[14] (Table VII). Both experiment and theory show a clear increase of complexation energy with the size of the alkane. As the bonds are electrostatic in nature, this reflects an increase in the polarizability (increasing the charge-induced dipole) and, to a lesser degree, a decrease in the ionization potential (IP) with the larger alkanes (allowing more charge transfer to the metal). This is significant because molecular complexes with the larger alkanes will have more internal energy to surmount the large barriers to insertion and elimination. As the IP continues to decrease with the size of the hydrocarbon and the polarizability continues to increase, reaction with Co^+ should become increasingly facile.

TABLE VII: Comparison of Our Calculated D_e Values and Best Estimates for $D_0°$ Values to the $D_0°$ Values Obtained through Equilibrium Measurements by Kemper, Bowers, and Co-workers[12,13] and Threshold Collisional Activation by Haynes and Armentrout[14] (in kcal/mol)

	theory		experiment ($D_0°$)	
	D_e[a]	$D_0°$[b]	ref. 13	ref. 14
$Co^+ + H_2$	18.3	17.4 ± 1	18.2 ± 1.0[c]	–
$Co^+ + CH_4$	21.4	22.7 ± 2	22.9 ± 0.7	21.4 ± 1.2
$Co(CH_4)^+ + CH_4$	23.1	24.4 ± 2	24.8 ± 0.8	23.3 ± 1.2
$Co^+ + C_2H_6$	25.0	26.4 ± 2	28.0 ± 1.6	24.0 ± 0.7
$Co^+ + C_3H_8$	29.3 ± 0.4	30.8 ± 2	–	30.9 ± 1.4

[a] For $Co(H_2)^+$, this is the MRCI + Q value. For all others, this is the MCPF value. [b] Our theoretical $D_0°$ values include a correction of 1 ± 1 kcal/mol for $Co(H_2)^+$ and 2 ± 2 kcal/mol for the metal–alkane complexes. These are conservative estimates of the errors introduced by limitations in the level of wave function, basis set, and geometry optimization. [c] Reference 12.

While the potential energy surfaces appear to be flat, there is a preference for coordination to C–H bonds. This coordination can be either η^2 (in which the alkane acts as a four-electron donor) or η^3 (in which it acts as a six-electron donor). Coordination is found to occur to C–H bonds on the same carbon center and on two different carbon centers. While this work is inconclusive as to whether there exists a preference for insertion into either primary or secondary C–H bonds, these results suggest that there is a bias toward insertion into C–H bonds rather than C–C bonds inherent in the molecular complex. In the case of $Co(C_2H_6)^+$ with C_2 symmetry, for instance, the bond is better described as η^2 coordination to two C–H bonds rather than coordination to the C–C bond.

Finally, we find that coordination of a second ligand is favorable. In the case of $Co(CH_4)_2^+$, the second bond is stronger than the first. This is due to the s-d hybridization that occurs on the metal upon complexation of the first methane. As this hybridization is appropriate for coordination of a second ligand, the second bond does not pay the cost of this hybridization. In addition, the nature of the hybridization and the charge transfer strongly favor the eclipsed D_{2h} geometry of $Co(CH_4)_2^+$ over the staggered D_{2h} geometry. The difference in energy between the two conformations was found to be 8.3 kcal/mol. In contrast, with η^3 coordination of the two methanes, the C–H bonds are staggered.

Acknowledgment. We gratefully acknowledge useful discussions with Paul Kemper, Petra van Koppen, and Michael Bowers (U.C. Santa Barbara) and appreciate the sharing of their work with us prior to publication. In addition, we thank Chris Haynes and Peter Armentrout (U. Utah) for sharing their work prior to publication. J.K.P. was supported in part by a fellowship from BP America (Jim Burrington). This research was partially supported by NSF-CHE-9100284, and the facilities of the Materials and Molecular Simulation Center were supported by grants from DOE/AICD, Allied-Signal, BP America, Asahi Chemical, Asahi Glass, Chevron, BF Goodrich, and Xerox.

References and Notes

(1) For a review, see: Eller, K.; Schwarz, H. *Chem. Rev.* **1991**, *91*, 1121.

(2) Tonkyn, R.; Ronan, M.; Weisshaar, J. C. *J. Phys. Chem.* **1988**, *92*, 92.

(3) (a) Byrd, G. D.; Freiser, B. S. *J. Am. Chem. Soc.* **1982**, *104*, 5944. (b) Irikura, K. K.; Beauchamp, J. L. *J. Phys. Chem.* **1991**, *95*, 8344.

(4) (a) Armentrout, P. B.; Beauchamp, J. L. *J. Am. Chem. Soc.* **1981**, *103*, 784. (b) Georgiadis, R.; Fisher, E. R.; Armentrout, P. B. *J. Am. Chem. Soc.* **1989**, *111*, 4251. (c) Jacobson, D. B.; Freiser, B. S. *J. Am. Chem. Soc.* **1983**, *105*, 5197.

(5) Hanratty, M. A.; Beauchamp, J. L.; Illies, A. J.; van Koppen, P.; Bowers, M. T. *J. Am. Chem. Soc.* **1988**, *110*, 1.
(6) (a) van Koppen, P. A. M.; Brodbelt-Lustig, J.; Bowers, M. T.; Dearden, D. V.; Beauchamp, J. L.; Fisher, E. R.; Armentrout, P. B. *J. Am. Chem. Soc.* **1990**, *112*, 5663. (b) van Koppen, P. A. M.; Brodbelt-Lustig, J.; Bowers, M. T.; Dearden, D. V.; Beauchamp, J. L.; Fisher, E. R.; Armentrout, P. B. *J. Am. Chem. Soc.* **1991**, *113*, 2359.
(7) Armentrout, P. B.; Beauchamp, J. L. *Acc. Chem. Res.* **1989**, *22*, 315 and references therein.
(8) (a) Janowicz, A. H.; Bergman, R. G. *J. Am. Chem. Soc.* **1982**, *104*, 352. (b) Janowicz, A. H.; Bergman, R. G. *J. Am. Chem. Soc.* **1983**, *105*, 3929. (c) Jones, W. D.; Feher, F. J. *J. Am. Chem. Soc.* **1982**, *104*, 4240. (d) Crabtree, R. H. *Chem. Rev.* **1985**, *85*, 245.
(9) Armentrout, P. B.; Georgiadis, R. *Polyhedron* **1988**, *7*, 1573.
(10) (a) Schilling, J. B.; Goddard, W. A., III; Beauchamp, J. L. *J. Am. Chem. Soc.* **1986**, *108*, 582. (b) Schilling, J. B.; Goddard, W. A., III; Beauchamp, J. L. *J. Phys. Chem.* **1987**, *91*, 5616.
(11) (a) Ohanessian, G.; Goddard, W. A., III *Acc. Chem. Res.* **1990**, *23*, 386. (b) Bauschlicher, C. W.; Langhoff, S. R. *Int. Rev. Phys. Chem.* **1990**, *9*, 149.
(12) Kemper, P. R.; Bushnell, J.; von Helden, G.; Bowers, M. T. *J. Phys. Chem.* **1993**, *97*, 52.
(13) Kemper, P. R.; Bushnell, J.; van Koppen, P.; Bowers, M. T. *J. Phys. Chem.* **1993**, *97*, 1810.
(14) Haynes, C. L.; Armentrout, P. B. Personal communication.
(15) (a) Schultz, R. H.; Armentrout, P. B. *J. Am. Chem. Soc.* **1991**, *113*, 729. (b) Schultz, R. H.; Armentrout, P. B. *J. Phys. Chem.* **1992**, *96*, 1662.
(16) Hill, Y. D.; Freiser, B. S.; Bauschlicher, C. W. *J. Am. Chem. Soc.* **1991**, *113*, 1507.
(17) Blomberg, M. R. A.; Siegbahn, P. E. M.; Svensson, M. *J. Am. Chem. Soc.* **1992**, *114*, 6095.
(18) Bauschlicher, C. W.; Partridge, H.; Langhoff, S. R. *J. Phys. Chem.* **1992**, *96*, 2475.
(19) (a) Das, K. K.; Balasubramanian, K. *J. Chem. Phys.* **1989**, *91*, 2433. (b) Das, K. K.; Balasubramanian, K. *J. Chem. Phys.* **1989**, *91*, 6254. (c) Das, K. K.; Balasubramanian, K. *J. Chem. Phys.* **1990**, *92*, 6697. (d) Das, K. K.; Balasubramanian, K. *J. Chem. Phys.* **1991**, *95*, 6880.
(20) Knight, L. B.; Cobranchi, S. T.; Herlong, J.; Kirk, T.; Balasubramanian, K.; Das, K. K. *J. Chem. Phys.* **1990**, *92*, 2721.
(21) (a) Dai, D.; Balasubramanian, K. *Chem. Phys. Lett.* **1991**, *185*, 165. (b) Balasubramanian, K.; Dai, D. *J. Chem. Phys.* **1990**, *93*, 7243. (c) Das, K. K.; Balasubramanian, K. *J. Chem. Phys.* **1991**, *94*, 3722.
(22) Zhang, H.; Balasubramanian, K. *J. Phys. Chem.* **1992**, *96*, 6981.
(23) (a) Alvarado-Swaisgood, A. E.; Harrison, J. F. *J. Phys. Chem.* **1985**, *89*, 5198. (b) Rappé, A. K.; Upton, T. H. *J. Chem. Phys.* **1986**, *85*, 4400.
(24) Mavridis, A.; Harrison, J. F. *J. Chem. Soc., Faraday Trans. 2* **1989**, *85*, 1391.
(25) (a) Schilling, J. B.; Goddard, W. A., III; Beauchamp, J. L. *J. Phys. Chem.* **1987**, *91*, 4470. (b) Rivera, M.; Harrison, J. F.; Alvarado-Swaisgood, A. *J. Phys. Chem.* **1990**, *94*, 6969.
(26) Rosi, M.; Bauschlicher, C. W.; Langhoff, S. R.; Partridge, H. *J. Phys. Chem.* **1990**, *94*, 8656.
(27) Berthier, G.; Cimiraglia, R.; Daoudi, A.; Mestdagh, H.; Rolando, C.; Suard, M. THEOCHEM **1992**, *254*, 43.
(28) (a) Chong, D. P.; Langhoff, S. R. *J. Chem. Phys.* **1986**, *84*, 5606. (b) Ahlrichs, R.; Scharf, P.; Ehrhardt, C. *J. Chem. Phys.* **1984**, *82*, 890.
(29) Hurley, M. M.; Pacios, L. F.; Christiansen, P. A.; Ross, R. B.; Ermler, W. C. *J. Chem. Phys.* **1986**, *84*, 6840.
(30) Perry, J. K.; Ohanessian, G.; Goddard, W. A., III *J. Chem. Phys.* **1992**, *96*, 7560.
(31) Huzinaga, S.; Sakai, Y. *J. Chem. Phys.* **1969**, *50*, 1371.
(32) Werner, H. J.; Meyer, W. *Mol. Phys.* **1976**, *31*, 855.
(33) Dunning, T. H. *J. Chem. Phys.* **1971**, *55*, 716.
(34) MOLECULE/SWEDEN is an electronic structure program system written by Almlöf, J.; Bauschlicher, C. W.; Blomberg, M. R. A.; Chong, D. P.; Heiberg, A.; Langhoff, S. R.; Malmqvist, P.-Å.; Rendell, A. P.; Roos, B. O.; Siegbahn, P. E. M.; Taylor, P. R.
(35) (a) Goddard, W. A., III, California Institute of Technology, unpublished manuscript. (b) Bobrowicz, F. W.; Goddard, W. A., III In *Modern Theoretical Chemistry: Methods of Electronic Structure Theory*; Schaefer, H. F., III, Ed.; Plenum Press: New York, 1977. (c) Bobrowicz, F. W. Thesis, California Institute of Technology, 1974, unpublished. (d) Ladner, R. C. Thesis, California Institute of Technology, 1972, unpublished. (e) Bair, R. A. Thesis, California Institute of Technology, 1982, unpublished.
(36) (a) Kubas, G. J.; Ryan, R. R.; Swanson, B. I.; Vergamini, P. J.; Wasserman, H. J. *J. Am. Chem. Soc.* **1984**, *106*, 451. (b) See also: Hay, P. J. *J. Am. Chem. Soc.* **1987**, *109*, 705.
(37) *Handbook of Chemistry and Physics*, 68th ed.; Weast, R. C., Ed.; Chemical Rubber Co.: Boca Raton, FL, 1987.
(38) Huber, K. P.; Herzberg, G. *Molecular Spectra and Molecular Structure IV. Constants of Diatomic Molecules*; van Nostrand Reinhold Co.: New York, 1979.
(39) Low, J. J.; Goddard, W. A., III *Organometallics* **1986**, *5*, 609.
(40) Blomberg, M. R. A.; Siegbahn, P. E. M.; Svensson, M. *J. Phys. Chem.* **1991**, *95*, 4313.
(41) Periana, R. A.; Bergman, R. G. *J. Am. Chem. Soc.* **1986**, *108*, 7332.
(42) Koga, N.; Morokuma, K. *J. Am. Chem. Soc.* **1990**, *94*, 5454.
(43) (a) Low, J. J.; Goddard, W. A., III *J. Am. Chem. Soc.* **1984**, *106*, 8321. (b) Low, J. J.; Goddard, W. A., III *J. Am. Chem. Soc.* **1984**, *106*, 6928. (c) Low, J. J.; Goddard, W. A., III *J. Am. Chem. Soc.* **1986**, *108*, 6115.
(44) Nicholson, A. J. C. *J. Chem. Phys.* **1965**, *43*, 1171.
(45) (a) Walch, S. P. Thesis, California Institute of Technology, 1977, unpublished. (b) Walch, S. P.; Bauschlicher, C. W. *J. Chem. Phys.* **1983**, *78*, 4597.